RSC Advances

PAPER

View Article Online
View Journal | View Issue

Cite this: *RSC Adv.*, 2023, **13**, 11337

Theoretical investigation of electrochromic mechanism in D–A conjugated polymers in visible and infrared bands†

Meiyu Zhang, Wencai Zhou, Biying Zhuang, Zilong Zheng, * Qianqian Zhang * and Hao Wang *

Electrochromic materials have been widely-applied in military camouflage and intelligent materials, in consideration of the multicolor display and infrared absorption. However, most of them have a narrow width of absorption spectra, and the electrochromic mechanism is still not well understood, especially in materials based on a copolymer structure in visible and infrared bands. Therefore, based on the polaron model, in order to enhance polarizability, we designed an "electronic donors–electronic acceptor" (D–A) type π-conjugated electrochromic polymer, which has an abundant color (wavelengths from 450 nm to 750 nm) with voltage range (from −0.2 V to 1.0 V). Employing first-principle calculations, we investigated the electrochromism of the polymer, which has a strong connection with the introduced new molecular orbital in the polaron (or cation), comparing with those in the neutral molecule. This study addressed the underlying mechanism for the electrochromic phenomenon and the behavior of the cation. It indicated the polaron molecular orbitals provide the photon absorption, whose energies are in the visible range and result in the electrochromic abundant color. In this work, we provide a molecular design for the adjustment of visible and infrared band absorption, which could have broad application in multicolor and infrared electrochromic materials.

Received 11th March 2023
Accepted 27th March 2023

DOI: 10.1039/d3ra01600e

rsc.li/rsc-advances

Introduction

Chromism is a process that refers to a change in a substance's color induced by various external stimuli, such as heating, lighting, and electric field. Electrochromism is the reversible change of a substance between the redox and oxidation states with distinguishable color induced by application of a potential difference.[1,2] The field of switchable electrochromic materials is constantly expanding,[3] with many new markets and technologies,[3] including smart windows,[2–5] anti-glare car mirrors,[4] dimming glass for cars or aircraft,[4] military camouflage,[6] flexible electronics,[3] and electrochromic displays.[4,7] Electrochromic materials can be divided into inorganic and organic species.[1] The inorganic materials have been widely used in the past decades, attributed to their high stability under working conditions.[1,2,8] In contrast to the widely studied inorganic electrochromic materials, the displayed color of organic materials is much easier to adjust considering the flexibility in molecular design.[9,10] Besides, organic materials have a more rapid color conversion, and reversibility with respect to inorganic ones.[10,11] However, the traditional organic electrochromic materials have the problem of narrow gamut.[10] Long-chain conjugated polymers have electrochromic effects, for instance, polythiophene,[12–14] polypyrrole,[15] polyaniline,[16] and polyfuran.[17]

The electrochemical doping can alter the π-conjugate structure, which induces changes in band gaps, and optical contrasts. The molecular design rules proposed by synthetic, experimental, and computational scientists have allowed for the rational control of molecular structure, in order to induce specific optoelectronic and conformational attributes. The design of molecular structure was confirmed by both theorical calculations and experimental measurement, which demonstrated the connection between optoelectronic property and molecular conformation.[17] The π-conjugated heterocyclic polymers are known for their tailorable optoelectronic properties. However, there is still lack of comprehensive researches on the rich color adjustment in π-conjugated polymers towards flexible electrochromic displays.[18] Especially, electrochromic mechanisms of multi-color tunability in the π-conjugated copolymers remain not well clear, which limits the reasonable designs of full-color materials.

In the field of conjugated polymer donor materials, polythiophene derivatives are the most important class of conjugated polymer donor materials. Webster research center in the United States first found that polythiophene has good electrochromic properties, however, the insolubility, poor processing

Faculty of Materials and Manufacturing, Faculty of Information Technology, Beijing University of Technology, Beijing, China. E-mail: zilong.zheng@bjut.edu.cn; zhangqianqian@bjut.edu.cn; haowang@bjut.edu.cn

† Electronic supplementary information (ESI) available. See DOI: https://doi.org/10.1039/d3ra01600e

performance limited its application in practical production. Therefore, many researchers start the study of polythiophene derivatives to overcome those shortcomeings.[19]

In the last few decades, many conductive polymers derivatives have been successfully prepared and their potential as advanced materials has been investigated.[20] Given the small structural modifications on the polymer backbone could make the band gap adjustment significantly, many methods have been used to improve the desired property. Recently, in order to obtain polymers with narrow bandgap, the electronic donor–acceptor (D–A) type materials have been focused, which have alternating electron-rich and electron-deficient groups in the backbone.[17,20] While the intramolecular charge transfer (ICT) state based on D–A structure can low the bandgap energy, driven with additional Coulomb interaction between donor fragment and acceptor fragment. Meanwhile, D–A structure could enlarge the polarization, which enhance the solubility and polaron generation of polymers in polar solution.

As electron-donor component of copolymer, poly(3,4-ethylenedioxythiophene) (PEDOT) is a polythiophene two-ring derivative with two alkoxy substituents attached to the 3- and 4-positions of the thiophene ring and linked by athylene. Electron-donating oxygen substituents stabilize free radicals and positive charges within the conjugated backbone, while six-membered ring closure with small spatial back difference extends stability.[21] Therefore, PEDOT presents good stability in the doped state, as well as high electrical conductivity through extended electron delocalization. PEDOT is synthesized by electrochemical polymerization, which tends to has positive charges, and compensated by the polymerized anion.[21] The doping level of PEDOT can be regulated by chemical or electrochemical redox reactions.[19] PEDOT can display three colors at different voltages, which are purple (at −0.8 V), light grey (at 0.2 V) and blue at (1.0 V).[19] 3,4-ethylenedioxythiophene (EDOT) is the electron donor unit, which can reduce the highest occupied molecular orbital (HOMO) level of the polymer by introducing strong electron-absorbing gethylene dioxythiopheneunit. Meanwhile, PEDOT has the advantages of high conductivity and good air stability.[18] As electron-acceptor component of copolymer, polypyrene (PPr) is also convenient for electrochemical copolymerization, whose initial oxidation potential is close to that of EDOT. Meanwhile, the pyrene containing copolymers can be used as hole transport materials.[22] Considering planar conjugated structure, pyrene containing compounds show strong intermolecular π–π interaction, which could be applied as sensitization unit by coupling with electron-rich moieties, for instance, thiophene and fluorene.[22] It is of great interest to investigate the conjugated effect and electrochemical property of copolymer, by combining electronic donor (EDOT) with electronic acceptor (pyrene).

The intramolecular charge transfer in D–A configuration can give rise to the change of absorption and bandgap energy. Here, we develop electrochromic π-conjugated copolymers based on a simple electrochemical copolymerization of 3,4-ethylenedioxythiophene (EDOT) and pyrene (Pr) monomers, which exhibit multi-color tunability behavior superior to the homopolymer of each monomer with single color. The modulation of energy-level configuration within the π-conjugated copolymers during doping process enables a dynamic and subtle color adjustment covering almost full colors.

The polaron model has been used for mechanism study of organic electrochromic molecules in the past decade.[18,23,24] With an external electric field, the charges are injected into the materials forming polaritons, and generate cations or free radicals following structural transformation. When an electron is removed from the organic chain, the electronic spin degeneracy is increased, and the gap orbitals of cation appear in the bandgap.[18,19] Under electric field, PEDOT derivatives could form free radical cations. The polarons and bipolarons are molecules with odd charges (+1, +3, +5) and even charges (+2, +4, +6), respectively,[19,25] while, bipolaritons are more stable than polaritons.[19,26] The electrochromic mechanism of π conjugated polymers is widely studied, however, the mechanism of ionization discoloration is not well clear.

We investigated the electrochromic mechanism in pure PEDOT, PPr and their copolymer. The electrochromic under the electrical field in the former can be attributed to two factors: (i) polaron molecular orbitals, which low the bandgap energy significantly; (ii) polaron-induced benzoquinone transition, which leads to chemical bond equalization with π electrons. The different charges on the polymer lead to the absorption band shift. Furthermore, the bandgap can be tunneled by controlling the geometrical configurations, the stoichiometric ratio of donor and acceptor, and the electric charge on the polymer. We have demonstrated a successful D–A configuration to construct conjugated organic backbone with reversible electrochromic properties that convert red to green, and provide a detailed guideline for the adjustment of infrared band absorption. We believe it will have broad application in a variety of EC devices.

Result and discussion

In order to match the absorption spectrum of the conjugated polymer to the visible spectrum, the absorption band of the polymer should be within the visible range (400–800 nm). Therefore, we first adjust the band gap range by molecular design.

Fig. 1 presented the correlation between the HOMO–Lowest Unoccupied Molecular Orbital (LUMO) gap based on modeling molecules. The investigated copolymers included D–A, A–A, and D–D conformations, as shown in Fig. 1a–c. Each of the conformations can have different connection sites and differences in *cis–trans* structures.[21] By calculating the relative system energy difference, the most stable structure is obtained from the lowest energy. The D/A ratio was further calculated to obtain the bandgap energy of the modeling D–A molecules. The PPr (A–A) exists 6 different configurations, while the PEDOT (D–D) has a difference in *cis*/*trans* structure. Therefore, both of them exist in their copolymer structure, leading to 5 different configurations. Different configurations lead to the change in the HOMO–LUMO gap. ΔE is equal to the maximum bandgap energy of the molecule minus the minimum bandgap energy, that is, the regulatory range of the bandgap energy. Surprisingly,

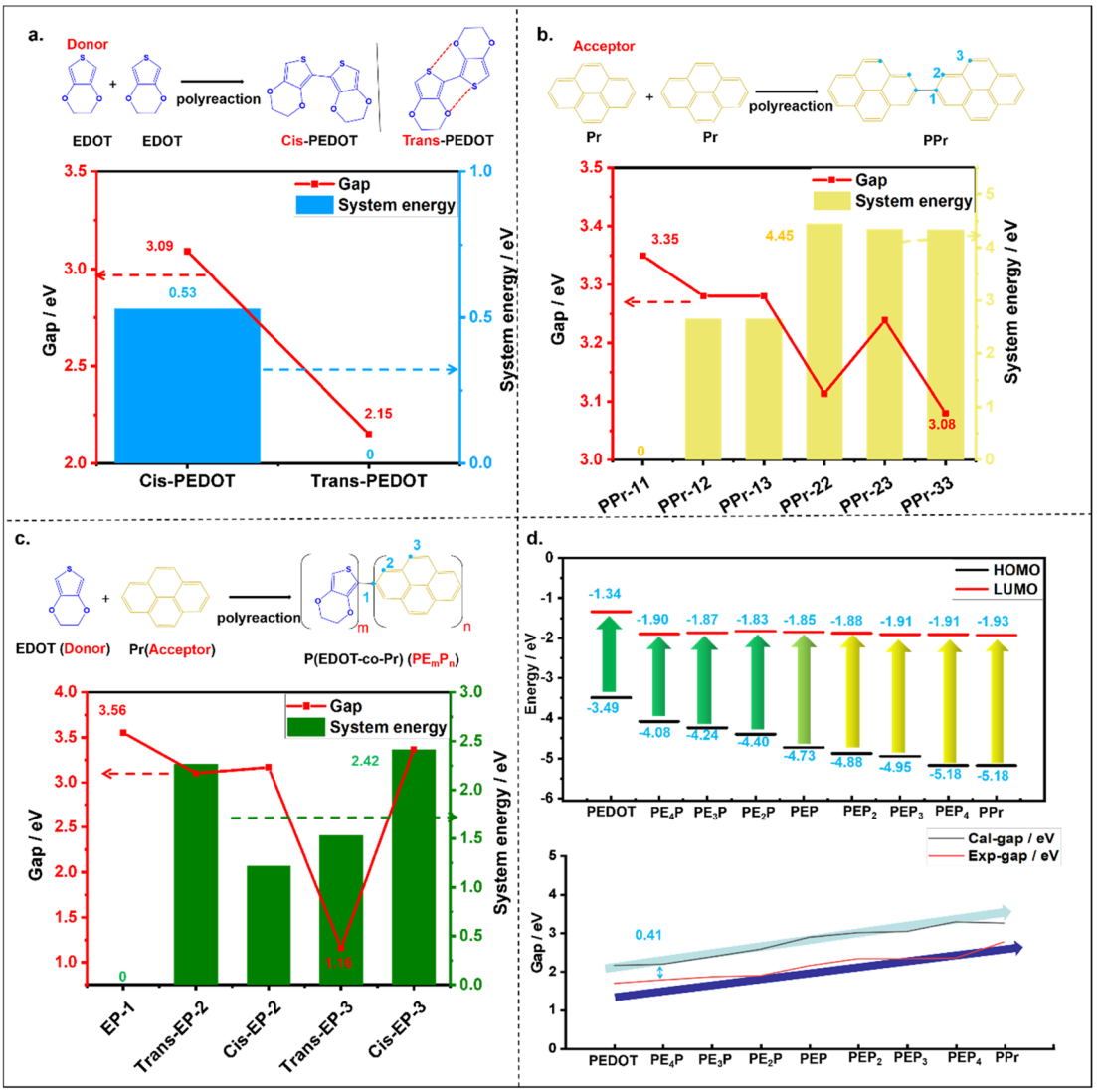

Fig. 1 System energy and bandgap energy. (a) System energy and bandgap energy in different conformations of PEDOT. (b) System energy and bandgap energy of PPr at different link sites. (c) System energy and bandgap energy of PEP at different link sites. (d) HOMO, LUMO and bandgap energy as a function of PEDOT/PPr ratios in copolymer.

different configurations of the copolymer resulting in a larger energy gap difference (ΔE is 2.4 eV), compared to the homopolymer (ΔE are 0.3 eV in PPr, and 0.94 eV in EDOT). The large value of the ΔE in the copolymer is from large overlapping between the electron and hole wavefunctions. In order to further figure out the most stable connection mode in the copolymer, we calculated the energy difference of all the connection sites (see Fig. 1). The calculated HOMO–LUMO gaps in the PEDOT and PPr are 2.15 eV and 3.25 eV, respectively, which agrees well with the experimental values. The proportional components adjust the range of HOMO and LUMO, which is 1.69 eV for HOMO and 0.59 eV for LUMO. It shows that different component proportions have a greater adjustment of HOMO. Then, we designed a series of copolymers based on these two materials with different concentration ratios of PE_mP_n. The values of m and n have a range from 0 to 4. We found that the change in the concentration ratio has a minor effect on the LUMO levels, while the HOMO level is shift down significantly, as the increase of the concentration ratio of the acceptor. The results indicated that the HOMO level is more sensitive to the concentration ratio than the LUMO level, which can be attributed to the large energy offset between HOMO levels. Consequently, the HOMO–LUMO gap was increased along with high concentration ratio of the acceptor, which is consistent with the experimental measurement. We noted that the calculated HOMO–LUMO gap values are 0.5 eV higher than the experiment, since the copolymers are with partial positive charges, which obtained from electrochemical polymerization and introduced the polaron band resulting in the low HOMO–LUMO gap.

By calculating the system energy and bandgap energy changes of molecules (see Fig. 1, S1–S4 and Table S1 in ESI†), we find the most stable and conjugated structures, and molecular structures with different positive charges are used to simulate

changes in molecules under an electric field. The total spin angular motion for the polaron and bipolaron systems are treated according to the experiment, with a spin of 1/2 and 0, respectively.[26] Fig. 2 presented the evolution of energy levels in various charged states. The results showed that the bandgap of cations is smaller than that of neutral molecules. The HOMO–LUMO energy gap of cations are decreased with more positive charges, since the additional charges introduce extra polaron molecular orbitals between HOMO and LUMO levels. The polarity of EP at different link sites remains stable with a molecular polarity index (MPI) of 12.7 kcal mol^{-1}, while that of charged PEDOT molecules continues to increase (MPI increases from 19 kcal mol^{-1} to 287 kcal mol^{-1}), see Tables S2 and S3 in ESI.†

As the charges increasing, the cation PEDOT have a benzoquinone transition during electrochromic process. The neutral *cis*-PEDOT has a higher bandgap energy than *trans*-PEDOT, because there is large special conjugated area in the former (see Fig. S5 in ESI†). The bandgap of cation (+2) *cis*-PEDOT smaller than that of *trans*-PEDOT, and the latter is energetically stable considering the additional O–S bond, while the O–S bond length is around 2.921 Å (see Fig. S6 in ESI†). Polarons odd positive charges produce single-occupied molecular orbitals (SOMO) with spin orbit energy splitting, rather than bipolarons with even positive charges. Therefore, the bandgap in the polariton structure is larger than that of bipolariton. The cations with more positive charges result in the rigid plane (see Fig. S7 and S8 in ESI†). In response to this phenomenon, the calculated O–S bond energy is 0.114 eV *via* isolated model, and there are 10 additional O–S bond in *trans*-structure of the modeling cation (+2) PEDOT with a polymerization of $n = 6$, which result in low molecular energy of 1.1 eV, see Fig. S6.† The energy difference between *cis*- and *trans*-configuration in neutral PEDOT is 0.53 eV, since the O–S bond number is increased with additional positive charge assistance, see Fig. S6 in ESI† and Fig. 1a.

PEP with D–A structure has the large dihedral angle adjustment range (16.1°) between each unit, which is only 0.54° in PEDOT (D–D structure). It implied the PEDOT have a plane structure and large conjugated system, as shown in Fig. 2d. The large dihedral angles could result in more spatial configurations, which lead to different absorption wavelength, it provides potential conditions for the molecule to absorb different color light. The higher the degree of oxidation, the more planar the molecules tend to be. It could be beneficial for charge transport, as we observe a simultaneous increase in electrochemical conductance upon polaron formation.[24]

Further analysis of cation behavior under simulated electric field conditions reveals the following changes. Form the bond distributions in Fig. 3, the electrostatic potential is rearranged with different carried charges, mainly in regions where π electrons change significantly (see Fig. S9 in ESI†). In the absence of

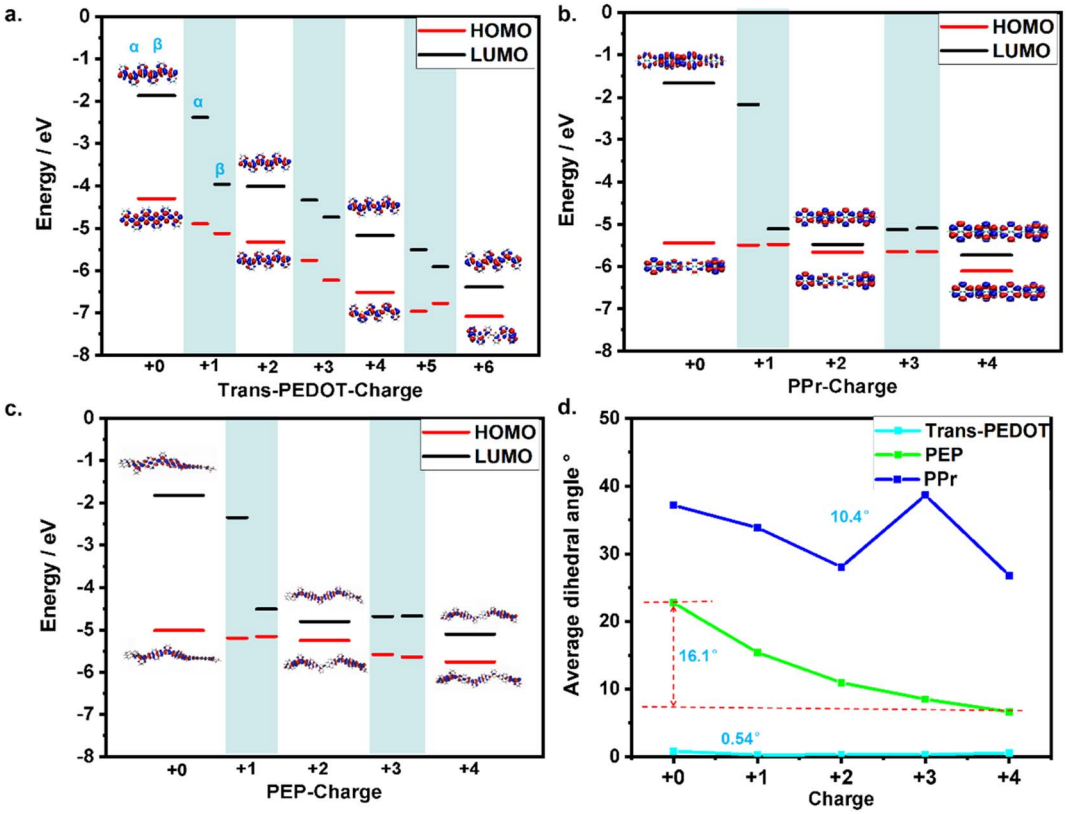

Fig. 2 HOMO and LUMO energy of cations. (a) HOMO and LUMO energy of *trans*-PEDOT (D–D) with positive charges of 0 to +6 charges. (b) HOMO and LUMO energy of PPr (A–A) with 0…+4 positive charges. (c) HOMO and LUMO energy of PEP (D–A) with 0…+4 positive charges. (d) Dihedral angles in D–A, A–A, and D–D with different positive charges.

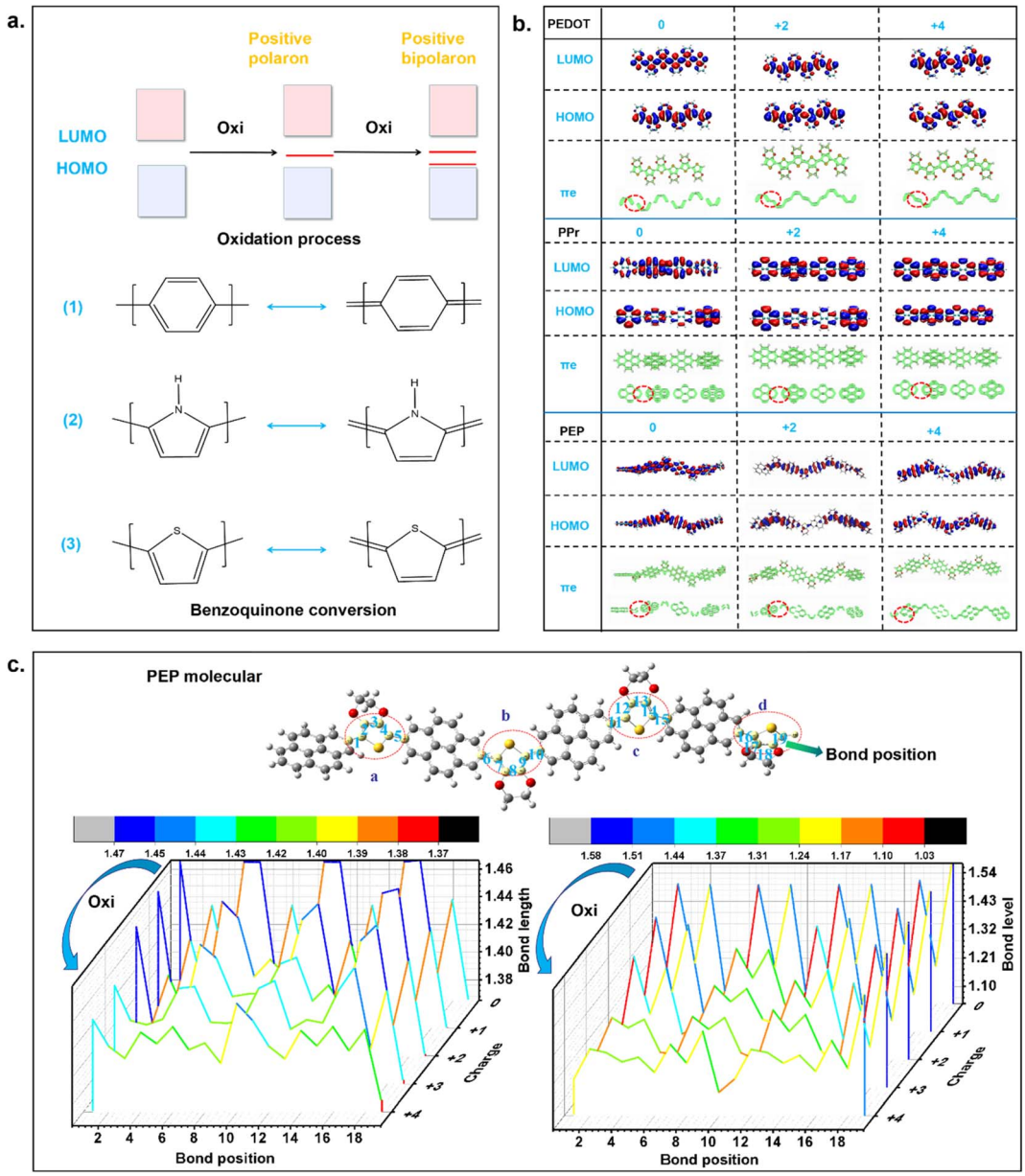

Fig. 3 The effect of the charges on molecular conjugation. (a) Benzoquinone conversion diagram of polaritons, and schematic diagram of the structure of benzoquinone conversion. (b) Charge distributions of π electrons during PEDOT, PPr and PEP electrochromic process and their HOMO–LUMO distribution. (c) Molecular structure, as well as, bond level and bond length of selected sites in PEP molecules with charges from 0 charges to +4 charges.

steric hindrance as the positive charge increases, the structure tends to keep planar geometry, and the more positive charge result in rigid molecular configuration. In Fig. 3, with more positive charges, conjugation planer leads to the equalization of both bond length and bond levels. The distribution of π electrons on the molecular chain varies with the amount of positive charges. Moreover, due to the inability of benzoquinone conversion between pyrene and pyrene, π electron cannot be connected. The pyrene link site can form a barrier to prevent from conjugation structure (see Fig. 3b and S10 in ESI†). Therefore, our molecular design was proposed to control the size of conjugation system by regulating the arrangement of fragment units.

Based on first-principles calculations, the perpendicular ionization potential (IP) was obtained, following the order of PPr (5.24 eV), PEP (4.76 eV), and PEDOT (3.99 eV). Under the same external electric field conditions, PEDOT is the most possible to form polaritons, and PPr is the worse one. The ionization potential can be regulated by the copolymerization ratio between EDOT and pyrene. The spatial overlap between HOMO and LUMO distributions decreases with the more fraction of pyrene component. The π electron transport pathway is along with intramolecular bond between EDOT and pyrene, see Fig. S11 in ESI.† The distribution of π electrons was obtained by strictly separating σ electrons from π electrons by localized molecular

orbitals (LMO). The negative electrostatic potential of neutral molecules is mainly contributed by π electrons. By analyzing its electrostatic potential, we found that the positive electrostatic potential originates from EDOT (see Fig. S11 in ESI†).

The absorption of visible and infrared wavelengths by charged molecules under the condition of electric field is simulated and verified. Fig. 4 presented the calculated absorption spectrum for the corresponding homopolymer and copolymer systems. The neutral PEDOT have a strong absorption at 551 nm (rendering purple-red), see Fig. 4b, agreed well with the experiment (red to purple),[27] completely undoped, neutral PEDOT is not blue, but red to purple (chemical synthesis). Therefore, the intense blue color must be attributed to polythiophene radical cations (polarons) in these layers, electrochemically polymerized molecules carry a small amount of charge, see Fig. 4a. The band in ultraviolet absorption is from the wavelength of 250 to 400 nm, which is the invisible light area. The spectrum of PEDOT (+1 to +4) is in the range of 419–582 nm, and its spectral variation trend is similar, only the intensity is different. At the same time, the first absorption peak of PEDOT (+1 to +4) is located before 419 nm, the range of the second absorption peak is 500–900 nm and the strongest absorption peak is located at about 600 nm, so PEDOT (+1 to +4) mainly absorbs red, orange and blue-violet, and shows a dark blue to light blue transition due to the change of absorption intensity, which is consistent with the experimental results (PEDOT has a wide and strong absorption peak between 500–900 nm and the color varies from dark blue to light blue).[28]

In PPr, the first peak at 318 nm keeps fairly unchanged between the eigenstate and oxidation states, and has slight absorption within 440 nm and beyond 600 nm (rendering light yellow-green),as shown in Fig. 4c which is consistent with the previous reports (331 nm and 348 nm).[28] In their copolymer PEP, the neutral had an absorption band around 441 nm in Fig. 4d (rendering red-orange), agrees well with the experiment in Fig. 4e (the absorption peak at −0.2 V is 436 nm). PEDOT

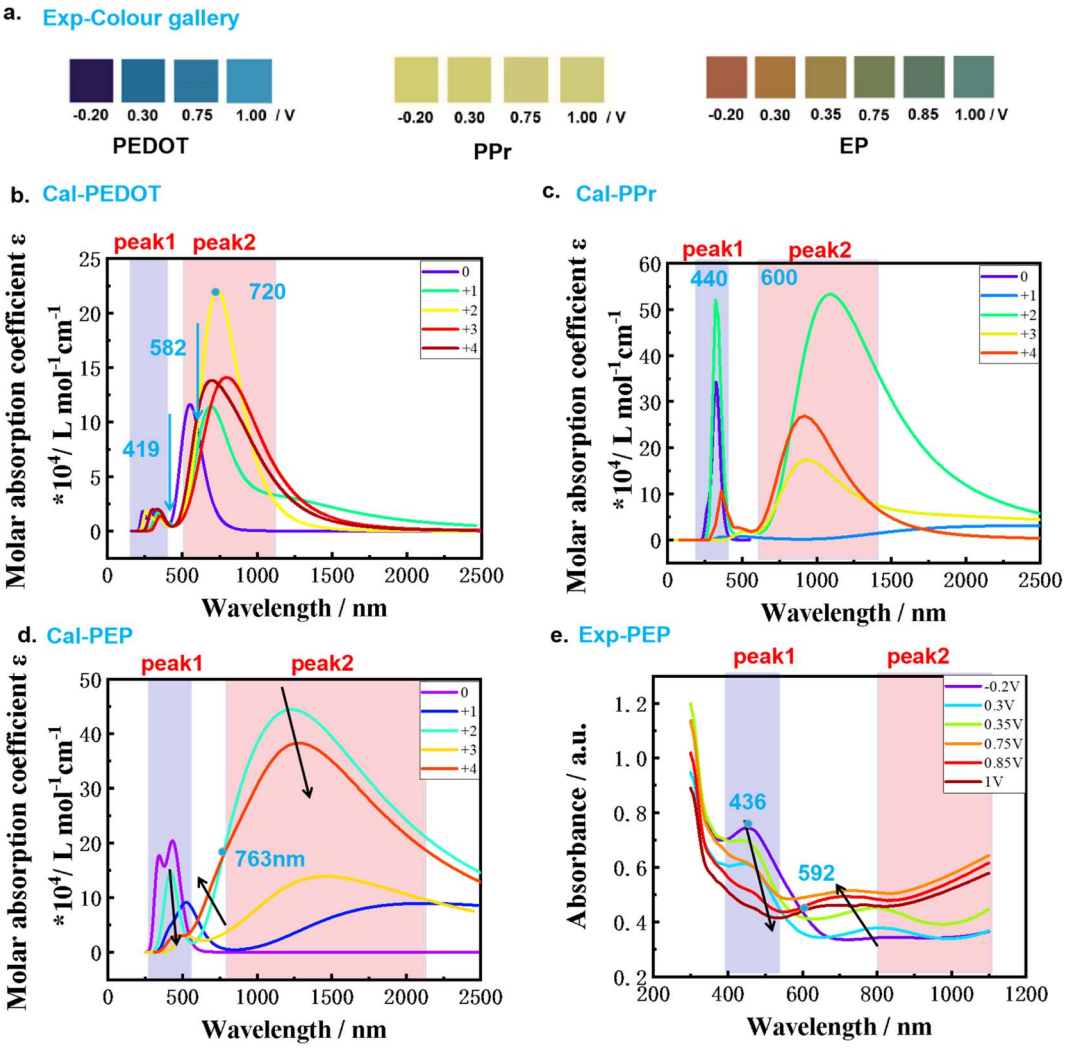

Fig. 4 Ionizing discoloration based on polaron mode. (a) Discoloration of PEDOT, PPr and PEP at different voltages. (b) Absorption spectra of PEDOT with charges from 0 to +6 charges. (c) Absorption spectra of PPr with charges from 0 to +4 charge. (d) Absorption spectra of PEP with charges from 0 to +4 charges. (e) Spectrum of PEP under an electric field.

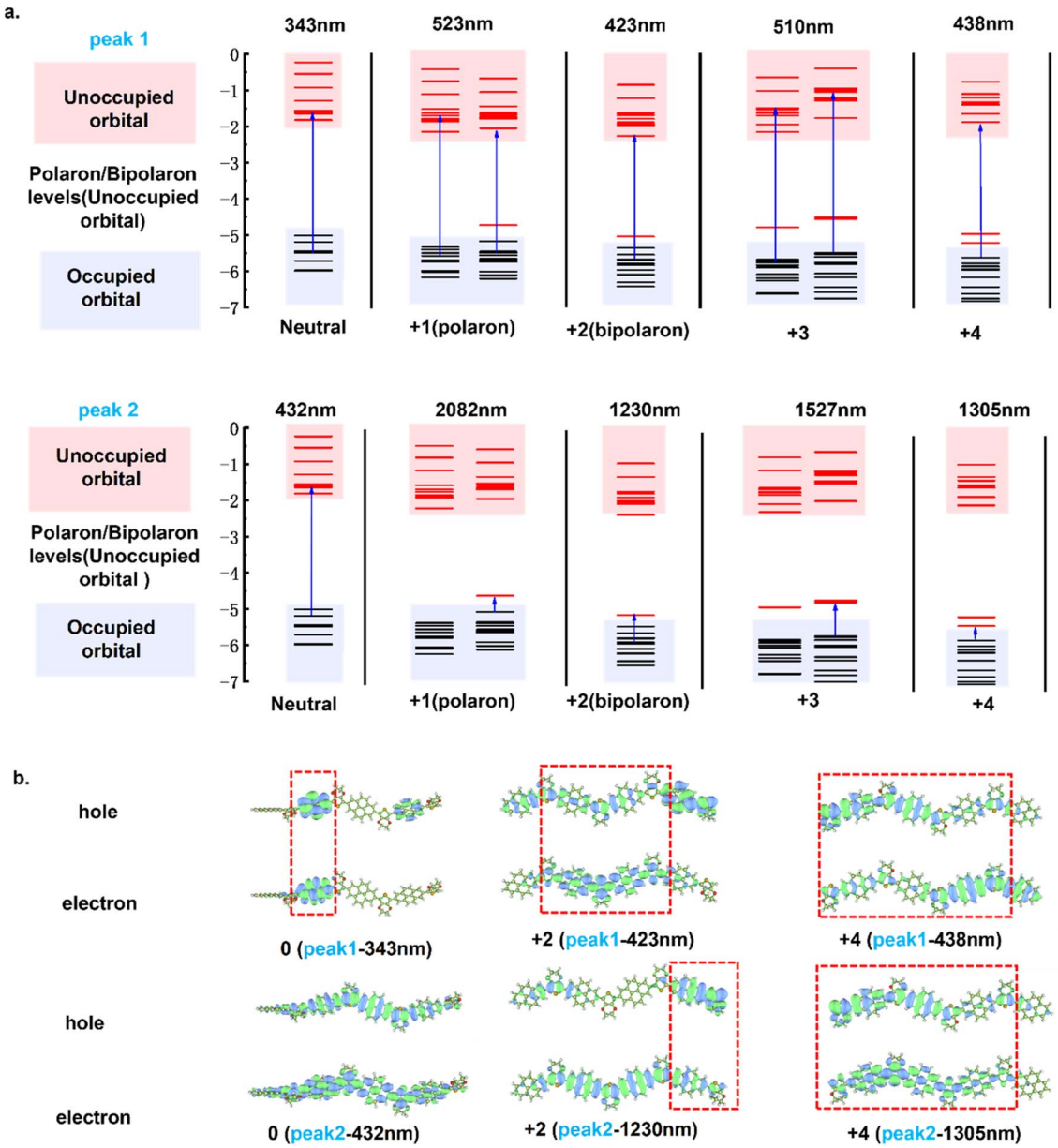

Fig. 5 Excited states of the strongest absorption band in PEP electrodiscoloration. (a) Excitation and the molecular orbital energy of PEP with 0…+4 changes at the strongest absorption band. (b) Natural transition orbital (NTO) of the strongest absorption band.

cation have one carrier type, which is the polaron. There are two types of polarons: polaron and bipolaron and the proportion of bipolaritons is more than 93%.[26] Therefore, the main electrodiscoloration of PEDOT is the absorption band different between bipolaron and neutral molecules. Besides, the results showed that both of the two bands (bipolarons: +2 and +4 charges) from the oxidation presented redshift character with a decreasing intensity, while the absorption range 500–763 nm goes blue-shift, see peak 1 in Fig. 4d and e, which is consistent with experiment (changes in absorption peak intensity and position). When the reduced state, PEP mainly absorbs the band of 400–600 nm, showing reddish-orange color. With the deepening of the degree of oxidation, it mainly absorbs between 600–700 nm, showing green.

PEDOT is more likely to form polaritons, and PPr is least likely to form them. Considering the first vertical ionization potential order with 3.99 eV, 4.76 eV and 5.24 eV of D–D, D–A and A–A structures (see Fig. S13 in ESI†), respectively. We found out the bipolaron is the primary key for the D–D and D–A copolymer,[26] considering the ionization potential order with 4.33 eV, 5.02 eV and 5.58 eV of D–D, D–A and A–A structures (see Fig. S13 in ESI†), respectively. While the large ionization potential of A–A polymer prevents from the generation of bipolaron, and result in the worse electrochromic capability. More importantly, the intramolecular charge transfer (ICT) based on D–A structure can low the bandgap energy, driven by additional Coulomb interaction between donor fragment and acceptor fragment, as well as reduce ionization potential. The

copolymerization ratio of EDOT/pyrene can benefit the bandgap energy control, and provide the mechanism multi-color electrochromic materials.

Further analysis of the strongest excited state in the absorption band in PEP electrochromism. As can be observed in Fig. 5a, the bandgap energies of cations have been significantly reduced from 3.2 eV to 0.31 eV, considering the inserted polaron molecular orbitals into the bandgap of neutral system. The absorption of infrared region is due to the low energy absorption caused by the downshift of the unoccupied orbitals energy which is mainly π–π^* transition from natural transition orbital (NTO) distributions. In the visible light region, the absorption peak position is changed slightly, with the wavelength shift of 15 nm (+2 to +4) and a similar molecular orbital transition. In combination with the electrostatic surface potential (ESP) analysis (see Fig. S9 in ESI†) the overlap between the electron and hole wavefunctions of the absorption band is localized at positive electrostatic potential region. The increase of spatial overlap result in the strong absorption band, for instance, the PEP cation with +2 and +4 charges; while the localized NTOs lead to less overlap and weak absorption band in PEP cation with +1 and +3 charges (see Fig. S12 in ESI†).

Conclusions

In the combination of the first-principle calculations with electrochemical preparation, we investigated bandgap energy and absorption band of "electronic donors–electronic acceptor" (D–A) electrochromic polymer. The effects of electrochromic conjugation configuration adjustment were studied including the copolymer connection, *cis–trans* structure, and charged cations. We found out the bipolaron is the primary key for the D–D and D–A copolymer, considering the ionization potential order with 4.33 eV, 5.02 eV and 5.58 eV of D–D, D–A and A–A structures, respectively. While the large ionization potential of A–A polymer prevents from the generation of bipolaron, and result in the worse electrochromic capability. More importantly, the intramolecular charge transfer (ICT) based on D–A structure can low the bandgap energy, driven by additional Coulomb interaction between donor fragment and acceptor fragment, as well as reduce ionization potential. The cationic behavior of electrostatic potential rearrangement, π electron distribution and bond length equilibrium introduced new polaron molecular orbital (of cation) and more benzoquinone sites, comparing with those in neutral molecule. Furthermore, both ICT and polaron molecular orbital result in low-energy fundamental gap and absorption band, and benzoquinone sites provide the possibility of abundant colors. It has broad application prospects in intelligent color-changing materials, infrared stealth in military and other fields.

Methodology

DFT calculations

The first-principle calculations were performed with density functional theory (DFT) *via* Gaussian 09 package. Considering DFT calculations performed on isolated systems do not account for electronic polarization, the polarizable continuum model (PCM) with the dielectric constant of 65.8 was applied for solvent effect of liquid environment, which consist of propylene carbonate (PC) and lithium perchlorate ($LiClO_4$). The modeling copolymer (PEP) was composed of both EDOT and pyrene monomers with a one-to-one ratio in our calculations. The positive charged polaron (+1*e*) and bipolaron (+2*e*) states in poly(3,4-ethylenedioxythiophene) (PEDOT) has been reported, which have the same monomer unit (EDOT) as one of those monomers (EDOT and pyrene) in copolymers PEP. Therefore, we investigated both neutral PEP, PEDOT, PPr and cation PEP, PEDOT, PPr in the simulations. The equilibrium structures of both neutral and cation PEP, PEDOT and PPr were obtained at the B3LYP/6-31G(d) level, and the excited state energies were calculated *via* conventional time-dependent DFT/PCM (TD-DFT/PCM) approach. The average dihedral angle, system energy and dipole moment of molecules were calculated through the Gaussian View. The natural transition orbitals (NTOs),[29] HOMO–LUMO electron cloud distribution, bond length and bond level, molecular polarity index (MPI), electrostatic surface potential (ESP)[30] and polishing orbital locator-π (LMO-LOL-π)[31] of both neutral and cation PEP were obtained *via* Multifwn code.[32]

Electrochemical and optical measurement

Preparation of P(EDOT-*co*-Pr) (PE_mP_n) films. The poly(EDOT-*co*-Py) were deposited on indium–tin-oxide-coated (ITO) glass *via* an electrochemical polymerization. All electrochemical polymerization is taken in $LiClO_4$-acetonitrile (ACN) solution containing different molar ratio (4 : 1, 3 : 1, 2 : 1, 1 : 1, 1 : 2, 1 : 3, 1 : 4) of EDOT and pyrene. The electropolymerization was performed with a Princeton Versa STAT 4 electrochemical workstation at room temperature and in a three-electrode system with the ITO glass/PET as the working electrode. After applying a constant potential of 1.2 V for a while, a blue-green thin film of PE_mP_n was formed on the substrate. During the measurement, the PE_mP_n (D–A) electrodes were served as working electrodes. A platinum wire and Ag/AgCl saturated with KCl were used as the counter and reference electrode, respectively. The electrolyte was 1.5 mol L^{-1} $LiClO_4$ in the solvent PC. The absorptivity spectra were collected by a PerkinElmer Lambda 900 UV-vis-near-infrared spectrophotometer.

Conflicts of interest

There are no conflicts to declare.

Acknowledgements

This work was supported by the National Science Foundation of China under Grant (No. 52073005, 22033006). National Natural Science Foundation of China (62075002).

References

1 D. Ma and J. Wang, *Sci. China: Chem.*, 2016, **60**, 54–62.

2 D. T. Gillaspie, R. C. Tenent and A. C. Dillon, *J. Mater. Chem.*, 2010, **20**, 9585.
3 C. M. Lampert, *Sol. Energy Mater. Sol. Cells*, 2003, **76**, 489–499.
4 C. M. Lampert, *Mater. Today*, 2004, **7**, 28–35.
5 G. A. Niklasson and C. G. Granqvist, *J. Mater. Chem.*, 2007, **17**, 127–156.
6 Z.-J. Li, C.-J. Yao and Y.-W. Zhong, *Sci. China: Chem.*, 2019, **62**, 1675–1685.
7 N. Vlachopoulos, J. Nissfolk, M. Möller, A. Briançon, D. Corr, C. Grave, N. Leyland, R. Mesmer, F. Pichot, M. Ryan, G. Boschloo and A. Hagfeldt, *Electrochim. Acta*, 2008, **53**, 4065–4071.
8 Z. Wang, X. Wang, S. Cong, J. Chen, H. Sun, Z. Chen, G. Song, F. Geng, Q. Chen and Z. Zhao, *Nat. Commun.*, 2020, **11**, 302.
9 W. Zhang, X. Wang, Y. Wang, G. Yang, C. Gu, W. Zheng, Y. M. Zhang, M. Li and S. X. Zhang, *Nat. Commun.*, 2019, **10**, 1559.
10 S. A. Jiang, J. L. Chang, J. W. Lin, Y. S. Zhang, T. S. Mo, J. D. Lin and C. R. Lee, *Adv. Opt. Mater.*, 2021, **9**, 2001796.
11 J. R. de Andrade, I. Cesarino, R. Zhang, J. Kanicki and A. Pawlicka, *Mol. Cryst. Liq. Cryst.*, 2014, **604**, 71–83.
12 R. B. Pernites, R. R. Ponnapati and R. C. Advincula, *Adv. Mater.*, 2011, **23**, 3207–3213.
13 R. Brooke, D. Evans, M. Dienel, P. Hojati-Talemi, P. Murphy and M. Fabretto, *J. Mater. Chem. C*, 2013, **1**, 3353.
14 H. Hayashi, A. Sobczuk, A. Bolag, N. Sakai and S. Matile, *Chem. Sci.*, 2014, **5**, 4610–4614.
15 A. Ghoorchian, F. Tavoli and N. Alizadeh, *J. Electroanal. Chem.*, 2017, **807**, 70–75.
16 F. Hu, J. Xu, S. Zhang, J. Jiang, B. Yan, Y. Gu, M. Jiang, S. Lin and S. Chen, *J. Mater. Chem. C*, 2018, **6**, 5707–5715.
17 W. Yao, L. Shen, P. Liu, C. Liu, J. Xu, Q. Jiang, G. Liu, G. Nie and F. Jiang, *Mater. Chem. Front.*, 2020, **4**, 597–604.
18 B. Yigitsoy, S. Varis, C. Tanyeli, I. M. Akhmedov and L. Toppare, *Thin Solid Films*, 2007, **515**, 3898–3904.
19 I. Petsagkourakis, N. Kim, K. Tybrandt, I. Zozoulenko and X. Crispin, *Adv. Electron. Mater.*, 2019, **5**, 1800918.
20 A. Balan, D. Baran and L. Toppare, *J. Mater. Chem.*, 2010, **20**, 9861.
21 Y. Nah, W. Choi and D. Kim, *Sol. Energy Mater. Sol. Cells*, 2008, **92**, 1547–1551.
22 Y.-C. Kung and S.-H. Hsiao, *J. Polym. Sci., Part A: Polym. Chem.*, 2011, **49**, 3475–3490.
23 A. De Sio, F. Troiani, M. Maiuri, J. Rehault, E. Sommer, J. Lim, S. F. Huelga, M. B. Plenio, C. A. Rozzi, G. Cerullo, E. Molinari and C. Lienau, *Nat. Commun.*, 2016, **7**, 13742.
24 I. Bargigia, L. R. Savagian, A. M. Osterholm, J. R. Reynolds and C. Silva, *J. Am. Chem. Soc.*, 2021, **143**, 294–308.
25 R. Ghosh and F. C. Spano, *Acc. Chem. Res.*, 2020, **53**, 2201–2211.
26 O. Bubnova, Z. U. Khan, H. Wang, S. Braun, D. R. Evans, M. Fabretto, P. Hojati-Talemi, D. Dagnelund, J. B. Arlin, Y. H. Geerts, S. Desbief, D. W. Breiby, J. W. Andreasen, R. Lazzaroni, W. M. Chen, I. Zozoulenko, M. Fahlman, P. J. Murphy, M. Berggren and X. Crispin, *Nat. Mater.*, 2014, **13**, 190–194.
27 S. Kirchmeyer and K. Reuter, *J. Mater. Chem.*, 2005, **15**, 2077.
28 C. Zhang, Y. Xu, N. Wang, Y. Xu, W. Xiang, M. Ouyang and C. Ma, *Electrochim. Acta*, 2009, **55**, 13–18.
29 Z. Liu, T. Lu and Q. Chen, *Carbon*, 2020, **165**, 461–467.
30 J. Zhang and T. Lu, *Phys. Chem. Chem. Phys.*, 2021, **23**, 20323–20328.
31 T. Lu and Q. Chen, *Theor. Chem. Acc.*, 2020, **139**, 25.
32 T. Lu and F. Chen, *J. Comput. Chem.*, 2012, **33**, 580–592.